Apical sparing pattern of left ventricular myocardial ^{99m}Tc-HMDP uptake in patients with transthyretin cardiac amyloidosis

Axel Van Der Gucht, MD, MSc,[a,b] Anne-Ségolène Cottereau, MD,[a,b] Mukedaisi Abulizi, MD,[a,b] Aziz Guellich, PhD,[a,c,d,e] Paul Blanc-Durand, MD, MSc,[a,b] Jean-Marc Israel, MD,[a,b] Arnault Galat, MD,[a,c,d,e] Violaine Plante-Bordeneuve, MD, PhD,[a,c,e,f] Jean-Luc Dubois-Randé, MD, PhD,[a,c,d,e] Diane Bodez, MD,[a,c,d,e] Jean Rosso, MD,[a,b,c] Thibaud Damy, MD, PhD,[a,c,d,e] and Emmanuel Itti, MD, PhD[a,b,c,e]

[a] Mondor Amyloidosis Network, Créteil, France
[b] Department of Nuclear Medicine, AP-HP, Henri Mondor Teaching Hospital, Créteil, France
[c] DHU ATVB, Paris Est University, Créteil, France
[d] Department of Cardiology, AP-HP, Henri Mondor Teaching Hospital, Créteil, France
[e] INSERM U955, GRC Amyloid Research Institute, Créteil, France
[f] Department of Neurology, AP-HP, Henri Mondor Teaching Hospital, Créteil, France

Received Dec 7, 2016; accepted Apr 5, 2017
doi:10.1007/s12350-017-0894-z

Background. **A decreased longitudinal strain in basal segments with a base-to-apex gradient has been described in patients with cardiac amyloidosis (CA).**

Objectives. **Aim was to investigate the left ventricular (LV) regional distribution of early-phase ^{99m}Tc-Hydroxymethylene diphosphonate (^{99m}Tc-HMDP) uptake in patients with transthyretin-related cardiac amyloidosis (TTR-CA).**

Methods. **All patients underwent a whole-body planar ^{99m}Tc-HMDP scintigraphy acquired at 10-min post-injection (early-phase) followed by a thorax SPECT/CT. The segmental uptake (expressed as % of maximal myocardial HMDP uptake) was investigated on the AHA 17-segment model and 3-segment model (basal, mid-cavity, apical).**

Results. **Sixty-one TTR-CA patients were included of whom 29 were wild-type (wt-TTR-CA) and 32 had hereditary TTR-CA (m-TTR-CA). Early myocardial ^{99m}Tc-HMDP uptake occurred in all TTR-CA. In all patients, segmental analysis of the LV myocardial distribution of ^{99m}Tc-HMDP uptake showed an increased median uptake (interquartile range) in basal/mid-cavity segments compared to the lowest median uptake of apical segments (respectively, 79% [72%-86%] vs. 72% [64%-81%]; $P < 10^{-6}$). This pattern was similar in wt-TTR-CA group (78% [70%-84%] vs. 70% [61%-81%]; $P < 10^{-6}$), in m-TTR-CA group (80% [74%-86%] vs. 73 [66%-82%]; $P < 10^{-7}$) and remained constant independently of the TTR mutation subtype with P ranging 10^{-5} to 0.03.**

Electronic supplementary material The online version of this article (doi:10.1007/s12350-017-0894-z) contains supplementary material, which is available to authorized users.

The authors of this article have provided a PowerPoint file, available for download at SpringerLink, which summarises the contents of the paper and is free for re-use at meetings and presentations. Search for the article DOI on SpringerLink.com

Axel Van Der Gucht and Anne-Ségolène Cottereau have contributed equally to this work.

Reprint requests: Axel Van Der Gucht, MD, MSc, Department of Nuclear Medicine, AP-HP, Henri Mondor Teaching Hospital, 51 Ave. du Mal de Lattre de Tassigny, 94010 Créteil, France; *axel.vandergucht@gmail.com*

1071-3581/$34.00

Conclusions. **Early-phase myocardial scintigraphy identified regional distribution of ^{99m}Tc-HMDP uptake characterized by a base-to-apex gradient, corroborating echocardiographic, and cardiac magnetic resonance findings. This apical sparing pattern was similar across TTR-CA and TTR mutation subtypes. (J Nucl Cardiol 2018;25:2072–9.)**

Key Words: SPECT/CT • HMDP • cardiac amyloidosis • transthyretin • protein deposition • apical sparing

Abbreviations	
AHA	American Heart Association
AL	Amyloid light-chain
CA	Cardiac amyloidosis
DPD	3,3-diphosphono-1,2-propanodicarboxylic
HMDP	Hydroxymethylene diphosphonate
LGE	Late gadolinium enhancement
LV	Left ventricular
MRI	Magnetic resonance imaging
PYP	Pyrophosphate
TTR	Transthyretin

See related editorial, pp. 2080–2083

INTRODUCTION

Cardiac amyloidosis (CA) is recognized as a cause of restrictive cardiomyopathy and heart failure consecutive to the accumulation of misfolded proteins in the myocardial interstitium.[1,2] The three most common types are light-chain (AL) amyloidosis due to excessive production of free immunoglobulin light chains secondary to an abnormal clonal proliferation of plasma cells, hereditary transthyretin amyloidosis (m-TTR) caused by various mutations in the TTR gene and wild-type transthyretin (wt-TTR) amyloidosis, known also as senile systemic amyloidosis, which occurs often after 60 years of age.[3]

Cardiac involvement is frequent in these main types of amyloidosis with a major impact on prognosis.[4] Early diagnosis of cardiac amyloidosis, as well as its typing, is of major clinical importance. Prognosis and therapeutic options vary strongly according to CA subtype. Several imaging modalities have been developed and proposed as noninvasive tools for the diagnosis of CA. A decreased longitudinal strain in basal segments with a base-to-apex gradient has been described at transthoracic echocardiography and late gadolinium enhancement (LGE) at cardiac magnetic resonance imaging (MRI).[5-9]

Myocardial uptake of bone tracers showed high sensitivity and specificity to diagnose TTR cardiac amyloidosis (TTR-CA) and differentiate it from AL amyloidosis.[10] We have shown recently that early-phase ^{99m}Tc-hydroxymethylene diphosphonate (^{99m}Tc-HMDP) scintigraphy perfectly predicts late-phase findings and has the advantage to be less time consuming, increase access to bisphosphonate scintigraphy, optimal for frail patients, and more interestingly, allows elimination of the bone tracer activity of ribs and sternum which could introduce errors in the evaluation of the ^{99m}Tc-HMDP myocardial uptake.[11] We have also shown that myocardial uptake intensity of ^{99m}Tc-HMDP is comparable to 3,3-diphosphono-1,2-propanodicarboxylic acid (DPD) which is the most widely used bone tracer in Europe.[12] Initially, scintigraphy imaging was based on whole-body scans, allowing only global analysis of the left ventricular (LV) ^{99m}Tc-HMDP distribution. Single-Photon Emission Computed Tomography/Computed Tomography (SPECT/CT) imaging allows for greater anatomic information, with the possibility to assess the uptake of each individual 17 segments. Then, aim of this study was to describe the pattern of regional myocardial distribution of ^{99m}Tc-HMDP uptake and to compare this pattern within the TTR-CA and TTR mutation subtypes.

METHODS

Study Population

Between October 2012 and March 2014, 61 patients followed in the Mondor Amyloidosis Network / GRC Amyloid Research Institute for a known TTR-CA were included. Inclusion criteria were age >18 years, coverage by the French statutory health insurance system, and absence of pregnancy. Data collection was approved by the Direction Interrégionale de la Recherche Clinique Ile-de-France (DC 2009-930) and by our local institutional review board. All patients provided written informed consent before study inclusion.

Diagnosis of Cardiac Amyloidosis

The diagnosis of TTR-CA was made as previously described.[13] Briefly, it was based on positive Congo-red and anti-TTR antibody staining of an endomyocardial or extracardiac biopsy specimen. When an extracardiac biopsy was negative and an endomyocardial biopsy was deemed ethically unacceptable due to advanced age, the diagnosis was made on the basis of different clinical findings including increased wall thickness at transthoracic echocardiography (>12 mm); increased N-terminal pro-brain natriuretic peptide, evidence from the medical history, and findings from the electrocardiogram and cardiac MRI. For all TTR amyloidosis, genetic sequencing of TTR was performed systematically to differentiate wt-TTR vs. m-TTR.

Early-phase ^{99m}Tc-HMDP Myocardial SPECT/CT

All patients underwent early-phase ^{99m}Tc-HMDP myocardial scintigraphy as part of their standard diagnostic workup.[11] No late-phase was performed as we have recently shown that early-phase scan was sufficient to diagnose TTR-CA. They were injected with an average 650 ± 14 MBq ^{99m}Tc-HMDP (Osteocis, IBA Molecular, Saclay, France) according to their body weight. Ten minutes later, early soft-tissue phase images were acquired using a dual-headed SPECT/CT camera equipped with low-energy high-resolution collimators (Precedence, Philips Healthcare, Da Best, The Netherlands). Acquisitions consisted of whole-body scan (20 cm/min) in the anterior and posterior views, followed by a tomographic acquisition, consisting of a standard helical CT (120 kV, 100 mAs, slice thickness 2.0 mm, 512 x 512 matrix) for anatomical correlation and attenuation correction, followed by a SPECT covering the thorax (120 projections, 20 s/projection, 1x zoom, 128 x 128 matrix).

Image Quantification

Image analysis was performed by an experienced nuclear physician and quality controlled by a senior nuclear physician blinded to histopathological and TTR gene sequencing results. SPECT image volumes were reconstructed using iterative reconstruction with CT-attenuation correction. They were carefully reoriented in the short-axis plane and bull's eye maps were obtained with the American Heart Association (AHA) 17-segment model, [14] using the QPS^{TM} software (Quantitative Perfusion SPECT, Cedars-Sinai Medical Center, Los Angeles, CA, USA).[15,16] Finally, the segmental uptake (expressed as % of maximal myocardial HMDP uptake) was investigated on the AHA 17-segment model and 3-segment model (basal, mid-cavity, apical).

Statistical Analysis

Values were expressed as mean ± SD or n (%) for population characteristics and median (25th-75th interquartile range) for segmental analysis of ^{99m}Tc-HMDP myocardial uptake. Comparison of variables was performed using the Mann-Whitney test. Comparison of the segmental uptake between TTR-CA and mutation subtypes was performed using unpaired t-test. Statistical analyses were performed using SPSS software (version 19.0 for Windows 2010, SPSS Inc., Chicago, IL, USA). P values < 0.05 were considered statistically significant. Interobserver reproducibility was determined by a second analysis of the segmental uptake on half of patients (27 randomized SPECT/CT scans) using the Kendall's coefficient of concordance (W).

RESULTS

Study Population

Table 1 summarizes clinical and echocardiographic characteristics of the study population. Sixty-one patients followed in our center for a known TTR-CA were included, of whom 32 had hereditary TTR-CA (m-TTR-CA) and 29 were wild-type (wt-TTR-CA). None of the patients had anti-TTR treatments prior to or during the study period. Amyloidosis was proved by (1) endomyocardial biopsy in 6 m-TTR and in 5 wt-TTR; (2) extracardiac biopsy in 19 m-TTR-CA and in 9 wt-TTR-CA. Seven patients with m-TTR-CA and 15 patients with wt-TTR-CA had negative extracardiac biopsy and for whom endomyocardial biopsy deemed unethical due to age, the diagnosis was made non-invasively based on echocardiography and cardiac MRI. The two most common mutations in the 32 patients with m-TTR-CA were Val122Ile ($n = 15$; 47%) and Val30-Met ($n = 6$; 19%). Other TTR mutations ($n = 11$; 34%) were Ala19Asp, Glu89Lys, Ile107Val, Leu68Ile, Thr49Ile, and Ser77Phe.

Early-phase ^{99m}Tc-HMDP Myocardial Uptake Depending on TTR-CA and Mutation Subtypes

Early myocardial ^{99m}Tc-HMDP uptake occurred in all TTR-CA. Examples are illustrated with ^{99m}Tc-HMDP planar images (Figure 1) and ^{99m}Tc-HMDP cardiac SPECT/CT images (Figure 2) of patients with m-TTR-CA and wt-TTR-CA. Data of segmental analysis of the ^{99m}Tc-HMDP myocardial uptake are listed in Table 2 and displayed using box-and-whisker plots in Figure 3. A good interobserver agreement was observed for basal, mid-cavity, apical segments and global cardiac uptake with Kendall's W values of 0.80, 0.87, 0.90, and 0.86, respectively. In all TTR-CA, segmental analysis of the ^{99m}Tc-HMDP myocardial uptake showed an increased median uptake (interquartile range) in basal/mid-cavity segments compared to the lowest median uptake of apical segments (respectively 79% [72%-86%] vs. 72% [64%-81%]; $P < 10^{-6}$). This pattern was similar in wt-TTR-CA group (78% [70%-84%] vs. 70% [61%-81%]; $P < 10^{-6}$) and m-TTR-CA group (80% [74%-86%] vs. 73% [66%-82%]; $P < 10^{-7}$). Interestingly, this regional distribution of ^{99m}Tc-HMDP uptake remained constant independently of the TTR mutation subtype (Table 2) with a higher median uptake in basal/mid-cavity segments compared to the lowest median uptake of apical segments in patients with Val122Ile mutation (respectively, 79% [73%-84%] vs. 72% [64%-80%]; $P < 10^{-5}$) and patients with other TTR mutations (82% [74%-86%] vs. 73% [67%-80%]; $P < 10^{-4}$). Although statistically significant, this pattern appeared less marked in patients with Val30Met TTR mutation (83% [75%-88%] vs. 81% [72%-85%]; $P = 0.03$) probably explained by the limited number of patients in this subgroup. Furthermore, in order to

Table 1. Population characteristics

Characteristics	Overall (*n* = 61)	wt-TTR-CA (*n* = 29)	m-TTR-CA (*n* = 32)	*P*
Clinical				
Age, years	76 ± 9	81 ± 6	71 ± 9	<0.001
Male sex, *n* (%)	49 (80)	26 (90)	23 (72)	0.08
Hypertension, *n* (%)	25 (41)	13 (45)	12 (38)	0.57
Canal tunnel syndrome, *n* (%)	33 (54)	14 (48)	19 (59)	0.39
Pacemaker or ICD, *n* (%)	34 (56)	12 (41)	22 (69)	0.03
NHYA class III-IV, *n* (%)	39 (64)	22 (76)	17 (53)	0.06
Neuropathy, *n* (%)	19 (31)	3 (10)	16 (50)	<0.001
ECG				
Microvoltage*, *n* (%)	15 (25)	5 (17)	10 (31)	0.52
PR duration, ms	215 ± 47	197 ± 42	226 ± 48	0.06
QRS duration, ms	110 ± 32	111 ± 33	109 ± 32	0.82
Atrial fibrillation, *n* (%)	26 (43)	16 (55)	10 (31)	0.06
Echocardiography				
LVEF, %	46 ± 13	44 ± 12	48 ± 14	0.21
IVST, mm	18 ± 4	18 ± 4	18 ± 4	0.98

Values are mean ± SD or n (%)
*Defined as QRS <5 mm in the limb leads and <10 mm in the precordial leads
ECG, electrocardiogram; *ICD,* implantable cardioverter-defibrollator; *IVST,* interventricular septal thickness; *LVEF,* left ventricular ejection fraction; *m-TTR,* hereditary transthyretin amyloidosis; *wt-TTR,* wild-type transthyretin amyloidosis; *CA,* cardiac amyloidosis

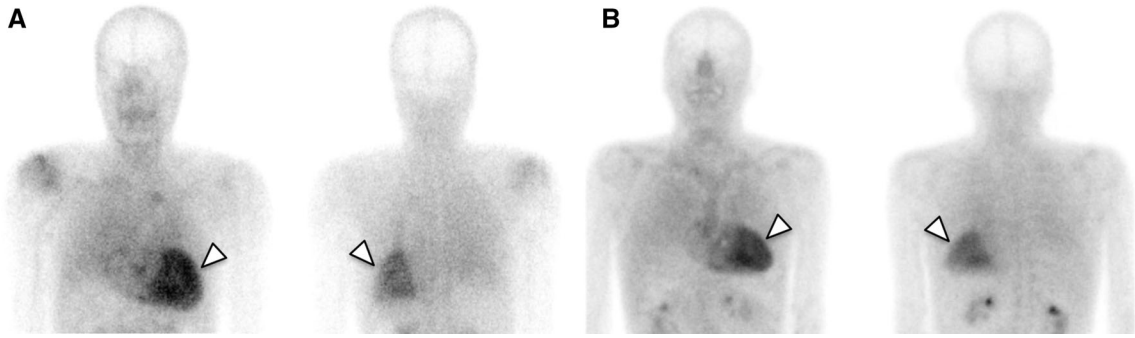

Figure 1. ^{99m}Tc-HMDP whole-body anterior and posterior planar views at early-phase scintigraphy showing a high myocardial ^{99m}Tc-HMDP uptake (*white arrowheads*) in a 82-year-old man with m-TTR-CA **(A)** and in a 79-year-old man with wt-TTR-CA **(B)**.

investigate the effect of attenuation correction, the segmental uptake % was calculated in attenuation-corrected (CTAC) and non-attenuation-corrected (NAC) images of 27 patients (21 wt-TTR-CA, 6 m-TTR-CA). Compared to NAC images, it was observed in CTAC images a slight decreased uptake of 5.6% ± 14% in apical segments and an increased uptake in basal (8.8% ± 17%) and mid-cavity segments (5.4% ± 14%).

DISCUSSION

The current study showed that ^{99m}Tc-HMDP using early myocardial SPECT/CT imaging is able to identify a myocardial pattern of ^{99m}Tc-HMDP uptake in TTR-CA and that this pattern was characterized by a base-to-apex gradient with an apical sparing of ^{99m}Tc-HMDP uptake. This apical sparing pattern was similar across TTR-CA and TTR mutation subtypes. The ^{99m}Tc-

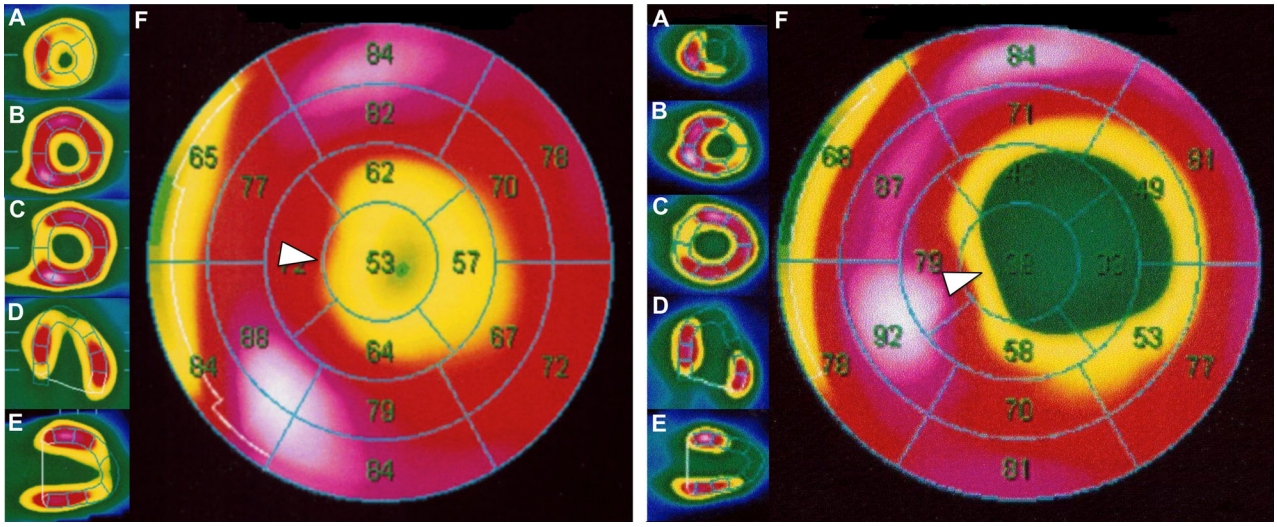

Figure 2. Early left ventricular myocardial ^{99m}Tc-HMDP uptake. Observe the base-to-apex gradient of ^{99m}Tc-HMDP uptake with an increased uptake in basal and mid-cavity segments compared to the lowest uptake of apical segments or apical sparing (*white arrowheads*) in a 78-year-old man with m-TTR-CA (left panel) and in a 82-year-old man with wt-TTR-CA (right panel). *A* Apical short axis (SA). *B* Mid-ventricular SA. *C* Basal SA. *D* Horizontal long axis (LA). *E* Vertical LA. *F* Bulls-eye map.

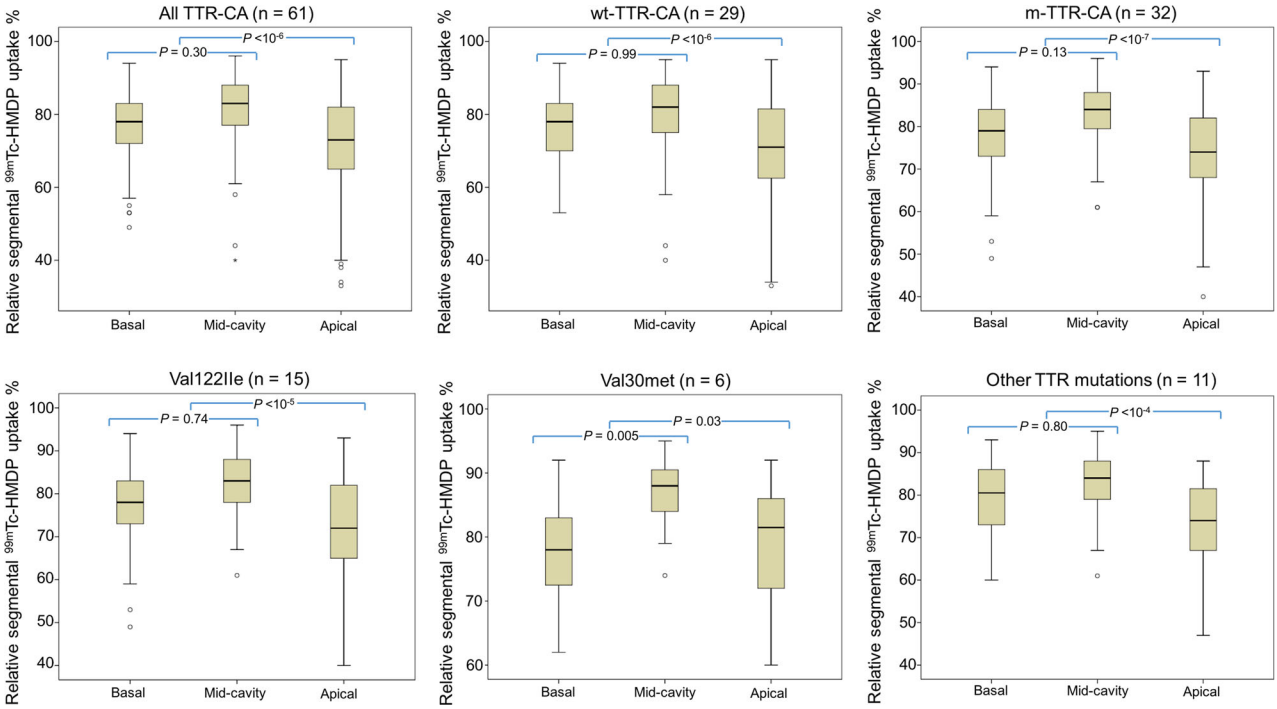

Figure 3. Box-and-whisker plots of segmental ^{99m}Tc-HMDP uptake (expressed as % of maximal myocardial HMDP uptake).

HMDP uptake of basal region was typically underestimated due to the smaller thickness of the basal membranous septum and basal inferior wall causes perfusion defect in the corresponding segments. Furthermore, compared to NAC images, we observed a small effect of attenuation correction with a small

Table 2. Segmental analysis of ^{99m}Tc-HMDP myocardial uptake (expressed as % of maximal myocardial HMDP uptake)

	wt-TTR-CA* (*n* = 29)	m-TTR-CA* (*n* = 32)	Val122Ile* (*n* = 15)	Val30Met* (*n* = 6)	Other mutations* (*n* = 11)
AHA 17-segment model					
1 - Basal anterior	80 (74-85)	83 (80-87)	80 (78-84)	82 (80-87)	86 (82-89)
2 - Basal anteroseptal	69 (62-75)	75 (70-79)	71 (70-75)	78 (72-80)	76 (74-81)
3 - Basal inferoseptal	78 (72-80)	79 (76-82)	79 (76-82)	76 (74-81)	77 (76-82)
4 - Basal inferior	81 (76-88)	83 (76-88)	82 (76-88)	85 (78-88)	83 (75-88)
5 - Basal inferolateral	74 (65-79)	74 (71-80)	74 (70-80)	75 (73-75)	75 (72-81)
6 - Basal anterolateral	76 (68-80)	76 (71-81)	76 (72-82)	71 (70-76)	76 (72-82)
7 - Mid anterior	74 (70-80)	80 (75-84)	76 (75-81)	88 (84-88)	80 (72-85)
8 - Mid anteroseptal	84 (78-87)	83 (81-88)	81 (81-87)	85 (81-88)	85 (82-88)
9 - Mid inferoseptal	87 (82-91)	89 (86-91)	89 (86-90)	90 (87-92)	87 (85-91)
10 - Mid inferior	82 (73-88)	84 (80-88)	83 (80-86)	88 (86-90)	83 (79-87)
11 - Mid inferolateral	70 (61-74)	73 (63-77)	72 (61-74)	77 (72-82)	71 (64-81)
12 - Mid anterolateral	69 (62-77)	72 (68-82)	70 (63-76)	81 (70-91)	74 (68-81)
13 - Apical anterior	67 (55-74)	73 (66-76)	72 (65-74)	77 (70-83)	71 (65-77)
14 - Apical septal	82 (78-85)	83 (74-86)	83 (75-86)	80 (74-86)	83 (74-86)
15 - Apical inferior	80 (69-88)	79 (71-83)	72 (69-82)	84 (81-87)	78 (71-81)
16 - Apical lateral	63 (51-69)	67 (59-73)	64 (56-68)	77 (67-85)	66 (59-74)
17 - Apex	65 (48-73)	68 (64-76)	67 (62-73)	78 (69-80)	68 (66-74)
3-segment model					
1 - Basal region (6 segments)	76 (68-81)	78 (73-82)	77 (72-82)	78 (73-82)	79 (74-84)
2 - Mid-cavity region (6 segments)	78 (70-86)	82 (74-87)	80 (73-86)	87 (81-89)	82 (75-87)
(Basal/mid-cavity regions)	77 (69-83)	80 (74-86)	78 (73-83)	82 (74-88)	81 (75-86)
3 - Apical region (5 segments)	70 (61-81)	73 (66-82)	72 (64-80)	81 (72-85)	73 (67-80)
P-value**	$<1.10^{-5}$	$<1.10^{-6}$	$<1.10^{-5}$	$<1.10^{-2}$	$<1.10^{-4}$

* Values are median (25th-75th interquartile range)
** Between ^{99m}Tc-HMDP uptake of basal/mid-cavity and apical segments based on 17-segment model
m-TTR, hereditary transthyretin amyloidosis; *wt-TTR,* wild-type transthyretin amyloidosis; *CA,* cardiac amyloidosis

decrease in the apical segments and a relative increase in the basal and mid-cavity segments. As stressed by Ficaro et al.[17] in their phantom study, attenuation correction (with an external radioactive source) allows to recover the low counts of inferior and basal walls and gives more accurate radioactive concentrations than NAC images. This probably reinforces the basal-to-apical gradient found in our study but does not create apical defects. Since bull's eye analysis is a relative quantification of uptake, it is expected that the increase of % uptake in the basal segments is compensated by a reduction of % uptake in apical segments which are more superficial and less attenuation corrected, as confirmed by the measurements given above. Moreover, we believe that attenuation correction will be increasingly used with hybrid SPECT/CT, PET/CT and more recently PET/MRI systems and will become a standard in nuclear cardiology.

Segmental Cardiac Uptake ^{99m}Tc-HMDP Gradient and Comparison with Other Techniques

Our findings which demonstrated a base-to-apex gradient of ^{99m}Tc-HMDP uptake are in line with previous work from us and other showing that amyloid burden predominates at the basal level using transthoracic echocardiography, cardiac MRI, and histopathological from explanted heart.[18] This is of importance as this study suggests that a correlation can be made between ^{99m}Tc-HMDP scintigraphy and transthoracic echocardiography or cardiac MRI concerning the segmental amyloid burden. Furthermore, this regional distribution of ^{99m}Tc-HMDP uptake seems to be similar with other bone tracer such as ^{99m}Tc-DPD,[12] and ^{99m}Tc-pyrophosphate (^{99m}Tc-PYP). In a recent study, Sperry et al. showed from a population of 35 patients with TTR-CA a gradient of

decreasing ^{99m}Tc-PYP uptake when progressing apically in the left ventricle, in parallel to the improvement in regional echocardiographic strain.[19] Furthermore, this reinforces the interest for using early-phase imaging with these bone tracers.

Usefulness of Quantifying Amyloid Burden Using ^{99m}Tc-HMDP

The diagnostic value of various bone tracers has been reported using conventional scintigraphy for distinguishing TTR-CA from other forms of CA.[20-23] We already demonstrated that ^{99m}Tc-HMDP was useful to differentiate TTR-and AL-CA as well as CA from non-amyloid causes of left ventricular hypertrophy and was able to provide prognostic information. Cardiac uptake of ^{99m}Tc-HMDP is increasing during the time in some patients suggesting that ^{99m}Tc-HMDP may be able to monitor the progression of the disease.[24] In this study, we showed that scintigraphy is able to quantify segmental and global cardiac tracer uptake in all types of transthyretin-related cardiac amyloidosis. To the best of our knowledge, this is the first research study quantifying ^{99m}Tc-HMDP cardiac uptake in TTR amyloidosis. Being able to determine quantitatively the progression of the disease by measuring segmental transthyretin-related cardiac amyloid burden at the segmental level may be of importance as several drugs are in development in TTR amyloidosis.[18] This will allow amyloid burden measurement and suggest that ^{99m}Tc-HMDP scintigraphy might be used as a surrogate endpoint in clinical trials to measure the response to treatment. Of course, further studies are needed to demonstrate the segmental progression of the disease using ^{99m}Tc-HMDP or other cardiac tracers.

NEW KNOWLEDGE GAINED

Our findings establish that scintigraphy is able to quantify segmental and global cardiac tracer uptake in all types of TTR-CA and might be used as a surrogate endpoint in clinical trials to measure the response to treatment.

CONCLUSION

Early-phase myocardial scintigraphy identified regional distribution of ^{99m}Tc-HMDP uptake characterized by a base-to-apex gradient of the LV ^{99m}Tc-HMDP uptake corroborating the gradient described in transthoracic echocardiography and cardiac MRI. This apical sparing pattern was similar across TTR-CA and TTR mutation subtypes.

Acknowledgments

We thank all the physicians involved in the Amyloidosis Network of the Henri Mondor Hospital who participated in the assessment and care of the patients included in this study.

Disclosure

The authors have indicated that they have no financial conflict of interest.

Ethical Approval

The procedure followed was in accordance with the ethical standards guidelines of the responsible committee on human experimentation.

References

1. Galat A, Guellich A, Bodez D, Slama M, Dijos M, Zeitoun DM, et al. Aortic stenosis and transthyretin cardiac amyloidosis: The chicken or the egg? Eur Heart J 2016;37:3525-31.
2. Damy T, Costes B, Hagège AA, Donal E, Eicher J-C, Slama M, et al. Prevalence and clinical phenotype of hereditary transthyretin amyloid cardiomyopathy in patients with increased left ventricular wall thickness. Eur Heart J 2016;37:1826-34.
3. Merlini G, Bellotti V. Molecular mechanisms of amyloidosis. N Engl J Med 2003;349:583-96.
4. Roig E, Almenar L, González-Vílchez F, Rábago G, Delgado J, Gómez-Bueno M, et al. Outcomes of heart transplantation for cardiac amyloidosis: Subanalysis of the spanish registry for heart transplantation. Am J Transpl 2009;9:1414-9.
5. Koyama J, Falk RH. Prognostic significance of strain Doppler imaging in light-chain amyloidosis. JACC Cardiovasc Imaging 2010;3:333-42.
6. Phelan D, Collier P, Thavendiranathan P, Popović ZB, Hanna M, Plana JC, et al. Relative apical sparing of longitudinal strain using two-dimensional speckle-tracking echocardiography is both sensitive and specific for the diagnosis of cardiac amyloidosis. Heart 2012;98:1442-8.
7. Fontana M, Banypersad SM, Treibel TA, Maestrini V, Sado DM, White SK, et al. Native T1 mapping in transthyretin amyloidosis. JACC Cardiovasc Imaging 2014;7:157-65.
8. Syed IS, Glockner JF, Feng D, Araoz PA, Martinez MW, Edwards WD, et al. Role of cardiac magnetic resonance imaging in the detection of cardiac amyloidosis. JACC Cardiovasc Imaging 2010;3:155-64.
9. Deux J-F, Damy T, Rahmouni A, Mayer J, Planté-Bordeneuve V. Noninvasive detection of cardiac involvement in patients with hereditary transthyretin associated amyloidosis using cardiac magnetic resonance imaging: A prospective study. Amyloid 2014;21:246-55.
10. Gillmore JD, Maurer MS, Falk RH, Merlini G, Damy T, Dispenzieri A, et al. Nonbiopsy Diagnosis of Cardiac Transthyretin Amyloidosis. Circulation 2016;133:2404-12.
11. Galat A, Van der Gucht A, Guellich A, Bodez D, Cottereau A-S, Guendouz S, et al. Early Phase (99)Tc-HMDP Scintigraphy for the Diagnosis and Typing of Cardiac Amyloidosis. JACC Cardiovasc Imaging 2016. doi:10.1016/j.jcmg.2016.05.007.
12. Abulizi M, Cottereau A-S, Guellich A, Vandeventer S, Galat A, Van Der Gucht A, et al. Early-phase myocardial uptake intensity of (99m)Tc-HMDP vs (99m)Tc-DPD in patients with hereditary

transthyretin-related cardiac amyloidosis. J Nucl Cardiol 2016. doi:10.1007/s12350-016-0707-9.

13. Bodez D, Ternacle J, Guellich A, Galat A, Lim P, Radu C, et al. Prognostic value of right ventricular systolic function in cardiac amyloidosis. Amyloid 2016;23:158-67.
14. Cerqueira MD, Weissman NJ, Dilsizian V, Jacobs AK, Kaul S, Laskey WK, et al. Standardized myocardial segmentation and nomenclature for tomographic imaging of the heart. A statement for healthcare professionals from the Cardiac Imaging Committee of the Council on Clinical Cardiology of the American Heart Association. Circulation 2002;105:539-42.
15. Germano G, Kavanagh PB, Waechter P, Areeda J, Van Kriekinge S, Sharir T, et al. A new algorithm for the quantitation of myocardial perfusion SPECT. I: Technical principles and reproducibility. J Nucl Med 2000;41:712-9.
16. Sharir T, Germano G, Waechter PB, Kavanagh PB, Areeda JS, Gerlach J, et al. A new algorithm for the quantitation of myocardial perfusion SPECT. II: Validation and diagnostic yield. J Nucl Med 2000;41:720-7.
17. Ficaro EP, Fessler JA, Ackermann RJ, Rogers WL, Corbett JR, Schwaiger M. Simultaneous transmission-emission thallium-201 cardiac SPECT: Effect of attenuation correction on myocardial tracer distribution. J Nucl Med 1995;36:921-31.
18. Ternacle J, Bodez D, Guellich A, Audureau E, Rappeneau S, Lim P, et al. Causes and Consequences of Longitudinal LV Dysfunction Assessed by 2D Strain Echocardiography in Cardiac Amyloidosis. JACC Cardiovasc Imaging 2016;9:126-38.
19. Sperry B, Vranian M, Tower-Rader A, Hachamovitch R, Hanna M, Jaber W. Apical Sparing Left and Right Ventricular Uptake of Technetium Pyrophosphate in Transthyretin Cardiac Amyloidosis. J Nucl Med 2016;57:172.
20. Rapezzi C, Quarta CC, Guidalotti PL, Pettinato C, Fanti S, Leone O, et al. Role of (99m)Tc-DPD scintigraphy in diagnosis and prognosis of hereditary transthyretin-related cardiac amyloidosis. JACC Cardiovasc Imaging 2011;4:659-70.
21. Worsley DF, Lentle BC. Uptake of technetium-99m MDP in primary amyloidosis with a review of the mechanisms of soft tissue localization of bone seeking radiopharmaceuticals. J Nucl Med 1993;34:1612-5.
22. Kulhanek J, Movahed A. Uptake of technetium 99m HDP in cardiac amyloidosis. Int J Cardiovasc Imaging 2003;19:225-7.
23. Glaudemans AWJM, van Rheenen RWJ, van den Berg MP, Noordzij W, Koole M, Blokzijl H, et al. Bone scintigraphy with (99m)technetium-hydroxymethylene diphosphonate allows early diagnosis of cardiac involvement in patients with transthyretin-derived systemic amyloidosis. Amyloid 2014;21:35-44.
24. Galat A, Rosso J, Guellich A, Van Der Gucht A, Rappeneau S, Bodez D, et al. Usefulness of (99m)Tc-HMDP scintigraphy for the etiologic diagnosis and prognosis of cardiac amyloidosis. Amyloid 2015;22:210-20.